

Biodegradable Intravascular (Gd-DTPA)-Cystamine Copolymer for Contrast Enhanced Magnetic Resonance Angiography: Initial Experience with Steady State Free Precession Acquisition in a Swine Model

T. D. Nguyen¹, P. Spincemaille¹, A. Vaidya², Z-R. Lu², Y. Wang¹

¹Radiology, Weill Medical College of Cornell University, New York, NY, United States, ²Pharmaceutics and Pharmaceutical Chemistry, University of Utah, Salt Lake City, UT, United States

INTRODUCTION

T1-shortening extracellular gadolinium (Gd) chelates such as Gd-DTPA and Gd-DOTA have revolutionized the quality of MR angiography (MRA), but are suitable for first-pass imaging only due to their rapid elimination from the blood pool after injection (1-3). Intravascular contrast agents have been developed to provide prolonged blood pool enhancement for time-consuming applications such as high-resolution and navigator 3D MRA (4-8). Recently a novel polydisulfide-based biodegradable contrast agent, (Gd-DTPA)-cystamine copolymers (GdCC), has been reported that provides extended blood pool retention and rapid renal clearance of toxic Gd(III) ions upon the breakdown of their macromolecular structures via the disulfide-thiol exchange reaction (9). This study evaluates the imaging performance of GdCC for balanced steady state free precession (SSFP) 3D MRA of the thorax in a swine model. We selected an SSFP-based sequence because it provides short repetition time, high blood signal-to-noise ratio (SNR), and excellent endogenous blood-to-myocardium contrast-to-noise ratio (CNR) for 3D cardiac MRI (10).

MATERIALS AND METHODS

Experiments were performed on six Yorkshire swines (mean weight of 35 ± 4 kg) using a 1.5 T GE SIGNA CV/i MR system. A four-element phased-array cardiac coil was used for signal reception. Each animal received an intravenous injection of 8-mL GdCC contrast agent (number average molecular weight $M_n = 15,000$ Da, weight average molecular weight $M_w = 17,000$ Da, ~ 0.1 mmol-Gd per kilogram of body weight) manually injected at a rate of 1 mL/s for 8 seconds followed by a 20-mL saline flush. Pre-contrast angiograms were acquired for comparison.

3D contrast-enhanced MRA of the thorax was acquired 15 seconds after the start of contrast injection during a 43-second breath-hold (respiratory ventilator off). The scanning parameters for the thoracic MRA pulse sequence (IR-prepared continuous 3D balanced SSFP) were: TR/TE/FA/rBW = 4.2 ms/1.4 ms/60°/±62.5 kHz, FOV = 26 cm, 2.4 mmx48 slices, in-plane resolution = 1.0x1.6 mm². Inversion pulses were inserted periodically into the RF trains such that data acquisition took place during the nulling of the background signals. A fan view ordering was used to optimize signal contrast and reduce eddy current artifacts (11). Immediately following the MRA of the thorax, 3D coronary MRA was obtained during free breathing. Due to pulse sequence and navigating system preparation, actual data acquisition started 3-3.5 minutes after the start of contrast injection. The scanning parameters for the coronary MRA pulse sequence (ECG-triggered segmented k-space balanced SSFP) were: TR/TE/FA/rBW = 4.2 ms/1.4 ms/60°/±62.5 kHz, FOV = 26 cm, 3 mmx16 slices, in-plane resolution = 1.0x1.0 mm², 16 partial echoes per heartbeat (corresponding to an acquisition window of 67 ms). An optimized magnetization preparation scheme that minimized the delay between the navigator and fat saturation pulses and the image echoes was used (12). For navigator gating, the PAWS gating algorithm (13), which optimizes gating window selection and minimizes residual motion artifacts within the gating window, was implemented on a Sun workstation that controlled data acquisition in real time. Motion bin size was 1 mm, corresponding to a gating window of 3 mm.

Blood and muscle signals (S_{blood} and S_{muscle}) were measured in adjacent areas of the ascending aorta and the chest wall. Noise standard deviation (σ_n) was estimated from the background air. Vessel SNR and CNR were defined as follows: $\text{SNR} = S_{\text{blood}}/\sigma_n$, $\text{CNR} = (S_{\text{blood}} - S_{\text{muscle}})/\sigma_n$. Two-tailed paired sample t-test was performed to determine the statistical significance of SNR and CNR differences between the pre-contrast and post-contrast angiograms.

RESULTS

All experiments were completed successfully except the breath-hold thoracic MRA in one pig due to pulse sequence problem. The measured blood SNR and blood-to-muscle CNR are summarized in Table 1. For background-suppressed 3D thoracic MRA (n = 5), the SNR and CNR of the post-contrast images were increased 23- and 90-folds, respectively, over the pre-contrast images ($p < 0.001$). Image comparison indicated that GdCC provided superior visualization of the thoracic vessel branches and the heart (Fig.1). For navigator 3D coronary MRA (n = 6), the SNR and CNR of the post-contrast images were significantly improved over the pre-contrast images by 18% and 20%, respectively ($p < 0.02$). Average scan times were 437 ± 135 seconds, indicating that GdCC had been effective over a prolonged imaging period. Fig.2 provided an example of image comparison, demonstrating that the new contrast agent markedly improved the depiction of the RCA (longer coronary segment and better vessel delineation).

DISCUSSION

The preliminary in vivo data have shown that the new contrast agent provides significantly improved quality for contrast-enhanced 3D SSFP imaging of the cardiovascular system. The increased blood residence time is particularly crucial for time-consuming navigator coronary MRA. Better SNR and CNR improvements for coronary MRA may be achieved with improved relaxivity and the use of preparation pulses such as inversion recovery or T2-prep.

REFERENCES

1. Prince MR et al. JMRI 1993;3:877-881.
2. Korosec FR et al. MRM 1996;36:345-351.
3. Goldfarb JW et al. Radiology 1998;206:830-834.
4. Li D et al. MRM 1998;39:1014-1018.
5. Grist TM et al. Radiology 1998;207:539-544.
6. Stuber M et al. JMRI 1999;10:790-799.
7. Huber ME et al. MRM 2003; 49:115-121.
8. Stillman AE et al. J Comput Assist Tomogr 1996;20:51-55.
9. Lu ZR et al. MRM 2004;51:27-34.
10. Spuentrup E et al. Invest Radiol 2003; 38:263-268.
11. Spincemaille P et al. MRM 2004;52:461-466.
12. Nguyen TD et al. MRM 2004;51:1297-1300.
13. Jhooti P et al. MRM 2000;43:470-480.

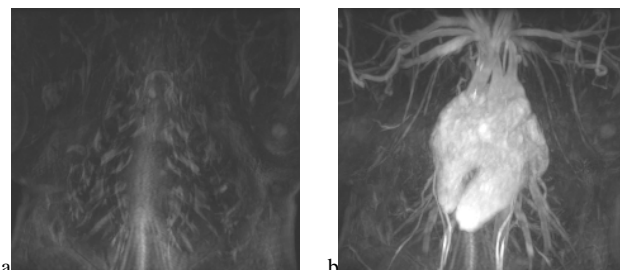


Fig.1. MIP images of thorax acquired with background suppression a) pre- and b) post-contrast. Markedly improved SNR is depicted in b.

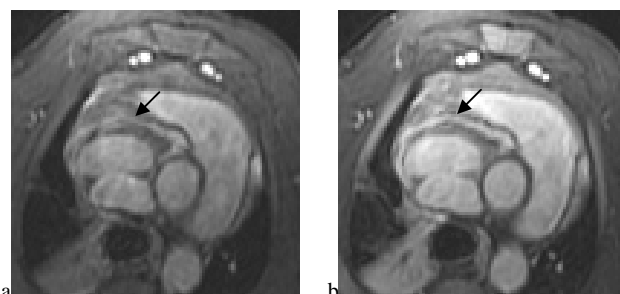


Fig.2. MIP images of RCA acquired a) pre- and b) post-contrast. Improved vessel delineation is depicted in b.

	SNR		CNR	
	pre	post	pre	post
Thoracic	6.2 ± 1.5	142.5 ± 17.0	1.5 ± 1.1	134.7 ± 15.0
Coronary	72.8 ± 4.8	86.0 ± 7.5	59.2 ± 4.8	70.6 ± 8.0

Table 1. SNR and CNR [mean \pm sd] comparison of pre-contrast and post-contrast thoracic (n = 5) and coronary (n = 6) 3D SSFP images.